Moringa (*Moringa oleifera*) leaves aqueous extract enhances fibronectin type III domain-containing protein 5 gene expression and serum irisin liberation in an obesity model

Reem K. Abdellah[a], Nadia M. El-Beih[a], Fatma A. Morsy[b], Khaled G. Abdel-Wahhab[c], Enas A. El-Hussieny[a]

[a]Department of Zoology, Faculty of Science, Ain-Shams University, Departments of [b]Pathology, [c]Medical Physiology, National Research Centre, Cairo, Egypt

Correspondence to Reem K. Abdellah, PhD, Department of Zoology, Faculty of Science, Ain-Shams University, Cairo, 11566, Egypt.
Tel: +20 100 240 706 00;
fax: (20) +2 684 78 24;
e-mail: reeemkamal@yahoo.com

Received: 15 September 2020
Revised: 4 October 2020
Accepted: 14 October 2020
Published: 26 March 2021

Egyptian Pharmaceutical Journal 2021, 20:92–103

Background
Obesity, a risk agent for many chronic diseases, leads to increased mortality and poses one of the major public health problems.
Objective
This study aimed to investigate the thermogenic and antiobese efficiency of Moringa aqueous extract (MAE) on obese-modeled rats.
Materials and methods
Adult male rats (150–170 g) were randomly divided into four groups, with 10 animals each, as follows: (a) healthy rats served as control, (b) healthy rats administrated with MAE (400 mg/kg/day), (c) obese-modeled rats, and (d) obese-modeled rats treated with MAE.
Results
After 30 consecutive days of treatment, the obtained results declared that MAE possessed antiobesity, thermogenic, antilipidemic, and antiinflammatory potential. MAE succeeded significantly in reduction of the BMI and serum leptin level coupled with up-regulation of fibronectin type III domain-containing protein 5 gene mRNA expression and serum irisin level. It clearly increased serum paraoxonase-1 activity and improved lipid profile values. Moreover, it markedly reduced serum tumor necrosis factor α and increased antioxidant activity, which was achieved from the marked improvement in malondialdehyde, nitric oxide, catalase, superoxide dismutase, and glutathione values in cardio-hepatic tissues. These findings were confirmed by the regeneration of the hepatic histopathological structure.
Conclusion
MAE, as a food supplement, could play a beneficial role in management of obesity and restoring its complications. This could be exhibited through multiple pathways, mainly via upregulation of fibronectin type III domain-containing protein 5 gene expression and production of the soluble myokine 'irisin,' which is responsible for browning of white adipose tissue as well as increment of total body energy expenditure.

Keywords:
fibronectin type III domain-containing protein 5 gene, irisin, Moringa, obesity, paraoxonase-1

Egypt Pharmaceut J 20:92–103

1687-4315

Introduction

With respect to the estimations of the WHO, more than 50% of the global adult population has obesity or is at least overweight [1]. In several areas worldwide, obesity abundance is still growing rapidly, and if the rate trends continue, it will record globally 18% in men and exceed 21% in women by 2025, inflicting severe burdens upon persons, societies, and health care system [2]. Depending on these statistics, obesity has been justifiably identified as a recent global epidemic health problem [3]. It is a risk agent for many chronic diseases, such as diabetes mellitus (type-2), nonalcoholic fatty liver disease, hypertension, hyperlipidemia, chronic kidney disease, cardiovascular disease, obstructive sleep apnea, osteoarthritis, and malignancies (e.g. breast, colon, and prostate), leading to increased mortality observed in obese individuals [4]. Thus, obesity poses one of the major public health problems nowadays and has a great relevance to both the health care system as well as individual health. Obesity is classically defined based on BMI, which is the anthropometric index that is widely used to identify obesity [5]. Contracting skeletal muscle secretes bioactive molecules called 'myokines.' One of the key molecules orchestrating many exercise-induced changes, including mitochondrial biogenesis and/or adipose tissue browning, is a transcription

cofactor, peroxisome proliferator-activated receptor-γ coactivator 1α (PGC1α) [6,7]. Interestingly, a link between myokines and PGC1α was recently discovered in the form of the new attractive PGC1α-driven myokine, irisin. Irisin was identified as a proteolytic cleavage product of the fibronectin type III domain-containing protein 5 (FNDC5), a transmembrane protein present mainly in skeletal muscle. In the original report by Boström *et al.* [6], FNDC5/irisin was induced by both PGC1α overexpression and physical activity in mice, and circulating irisin was shown to increase in humans in response to exercise. The evidence from *in vitro* and animal studies suggested the induction of the brown fat-like phenotype by FNDC5/irisin. Furthermore, an overexpression of FNDC5 gene in animal models of obesity resulted in marked up-regulation of uncoupling protein 1 and several mitochondrial genes, increase in oxygen consumption, amelioration of glucose tolerance, and reduction of insulinemia, demonstrating a greatly improved metabolic profile, most likely via elevated energy expenditure [6].

For many obese individuals, diet and behavioral modification need to be supplemented by pharmacotherapy, or increasingly, bariatric surgery, because attempted adherence to a balanced diet and healthy lifestyle has not addressed this problem [8]. At present, because of dissatisfaction with high costs and potentially hazardous adverse effects, the potential of natural products for treating obesity is under exploration, and this may be an excellent alternative strategy for developing future effective and safe antiobesity drugs [9]. A variety of natural products, including crude extracts and isolated compounds from plants, can induce body weight reduction and prevent diet-induced obesity [10]. One of those natural herbs is *Moringa oleifera*, which is known as Moringa in the literature, belonging to the family *Moringaceae*. It has been used for many health benefits [11]. *M. oleifera* is the most-studied and used species owing to its high phytochemical and pharmacological properties close to human health. It is largely cultivated in tropical and subtropical areas. Moringa is also usually defined as 'horseradish tree' or 'drumstick tree' [12]. As its leaves are rich in nutrients, especially vitamins and proteins, they can be cooked or eaten fresh to be used for prevention of malnutrition in populations [13]. It is commonly known as miracle tree, as various parts of the plant including roots, leaves, and seeds possess various medicinal as well as nutritional values. Therefore, various preparations of *M. oleifera* exhibited antibiotic, hypotensive, antiulcer, antiinflammatory, and anticancer properties [14]. The edible leaves of *M. oleifera* tree have been known as an antidiabetic food for centuries [15]. The aqueous extract of *M. oleifera* leaves demonstrated potent antioxidant and antidiabetic activity [16]. The pharmacological effects of its leaves have been reasoned to the synergistic actions of the different bioactive constituents included in its leaves that involve trace elements, vitamins [17], alkaloids (moringinine), carotenoids (β-carotene), and essential amino acids [18]. Moreover, *M. oleifera* contains three structural classes of phytochemicals with medicinal benefits, that is, glucosinolates (glucomoringin), flavonoids (quercetin and kaempferol), and phenolic acids [15]. It was reported that these phytochemicals possess antioxidant, antihyperglycemic, antihypertensive, lipid-lowering, anticancer, and antiinflammatory characteristics [18,19]. In addition, leaves of this plant are rich source of riboflavin, nicotinic acid, folic acid, and pyridoxine; therapeutically, these leaves are known to have antiatherosclerotic, tumor-suppressive, immune-boosting, and cardiovascular disease-preventive properties [20]. This study aimed to investigate the antioxidant exhibition of the aqueous extract of Moringa leaves *in vitro*; to explore Moringa aqueous extract (MAE) effect on the expression of FNDC4 gene (responsible for irisin secretion); and to interpret the relation among irisin level and paraoxonase-1 (PON1) activity with the obesity anthropometric and biochemical markers in obese-modeled rats in a trial to evaluate the obesity-modulating role of MAE as well as its lipid-lowering, antiinflammatory, and antioxidant efficiencies.

Materials and methods

Plant materials and extraction

Moringa (*M. oleifera*) herb was obtained from a local supplier (Abd El-Rahman Harraz, Bab El-Khalk Zone, Cairo, Egypt). It was identified and authenticated by scientific botanists at Botany Department, National Research Center and found carrying a taxonomic serial number 503874. The aqueous extract of dry Moringa leaves was carried out according to the method of Berkovich *et al.* [21]. In brief, 50 g of powdered dry leaves was soaked in 500 ml of distilled water and placed in a warm water bath (70°C) for 2 h, and then filtered through sterile filter paper (Whatman number 42, Whatman International Ltd, Maidstone, England). After lyophilization, the dry yield was stored at −20°C till use.

Determination of total phenolic content

Phenolic content of the MAE was performed by dissolving 5 mg of the extract in a 10-ml mixture of

acetone and water (6 : 4 v/v). Then, a sample of 0.2 ml was mixed with 1.0 ml of Folin-Ciocalteu reagent (10 fold diluted) and 0.8 ml of sodium carbonate solution (7.5%). After 30 min at room temperature, the absorbance was measured at 765 nm using Cary 100 ultraviolet–visible spectrophotometer. Estimation of phenolic compounds as catechin equivalents was carried out using standard curve of catechin [22].

DPPH radical scavenging activity

The capacity of antioxidants of MAE to quench DPPH radical was determined as previously described [23]. In this method, a certain amount (0.2 g) of the crude extract was dissolved in methanol to obtain a concentration of 200 ppm. A volume of 0.2 ml of this solution was completed to 4 ml by methanol, and 1 ml DPPH solution (6.09×10^{-5} mol/l), in the same solvent, was then added. The absorbance of the mixture was measured at 516 nm after 10-min standing. The reference sample (blank) was 1 ml of DPPH solution and 4-ml methanol. Triplicate measurements were made, and the percentage of radical scavenging activity was calculated according to the following equation:

$$\text{RSA}\ (\%) = \left(\frac{A_{\text{control sample}} - A_{\text{sample extract}}}{A_{\text{control sample}}} \right) \times 100.$$

Reducing power assay

The ferric ion (Fe^{3+})-reducing ability of MAE was assessed according to the method of Sethiya *et al*. [24], with slight modification. In this method, 0.5 ml of different fractions (50, 100, 200, 400, and 800 μg/ml) was mixed with 2.5 ml of phosphate buffer (pH 7.4) and 2.5 ml of potassium ferricyanide (0.1 M). This mixture was kept at 50°C in water bath for 20 min. After cooling, 2.5 ml of trichloroacetic acid (10%) was added and centrifuged at 3000 rpm for 10 min. Then, 2.5 ml of upper layer of the solution was mixed with 2.5 ml of distilled water and 0.5 ml of a freshly prepared ferric chloride solution (40% w/v). The absorbance of both sample and control (without samples) was measured at 700 nm. Ascorbic acid at various concentrations was used as standard, and the reducing power was calculated as equivalent to ascorbic acid from the standard curve.

Animals and induction of obesity

A total of 40 adult male Wistar albino rats (*Rattus norvegicus*) weighing 150–170 g were obtained from Animal Colony, National Research Center, Cairo, Egypt. The animals were housed in suitable plastic cages 1 week before the experimental study for acclimatization. Excess tap water and standard rodent food pellets [20.3% protein (20% casein and 0.3% DL-Methionine), 5% fat, 5% fiber, 3.7% salt mixture, and 1% vitamin mixture], obtained from Meladco Company for animals and rodents food pellets, El-Obour City, Cairo, Egypt, were always available. All animals received humane care in compliance with the standard institutional criteria as cited by animal ethical committee number FWA00014747, National Research Center. After the animals were acclimatized, the rats were fed for 3 months on a high-fat diet (raising standard rodent diet fat to 46% by corn oil, lard, and cholic acid). The weight and nose-anus length of each rat were measured at the end of the 3 months, and BMI was calculated by dividing the weight (g) by the square of nose-anus length (cm^2) [25]. Animals with BMI greater than 0.68 g/cm^2 were considered obese [26].

Experimental design

After induction of obesity, both normal and obese rats were randomly divided into four groups (10 rats each) as follows: (a) healthy or control animals, (b) healthy animals orally received a freshly prepared MAE (400 mg/kg/day) dissolved in distilled water for 4 weeks, (c) obesity-modeled animals without any treatment, and (d) obesity-modeled animals orally treated with MAE (400 mg/kg/day) for 4 weeks.

Blood and tissue sampling

At the end of the experimental period, the animals were fasted overnight, and following diethyl ether anesthesia, blood specimens were withdrawn from the retro-orbital plexus into vacutainer and centrifuged. Then the sera were separated, divided into aliquots, and stored at −80°C until biochemical measurements could be carried out as soon as possible. After blood collection, the animals were rapidly killed and parts of the liver and the heart of each animal were dissected, washed with saline, dried, and homogenized for tissue determinations of oxidative stress markers. Another part of the liver was soaked in formalin-saline buffer (10%) for microscopic examination. Vastus lateralis (muscle tissue) biopsies were taken, rolled in aluminum foil, and preserved at −80°C until molecular quantification of FNDC5 gene expression of irisin [27].

Tissue homogenate preparation

A specific weight (0.3 g), from either liver or heart, was homogenized in 3 ml of ice-cold phosphate buffer (50 mM, pH 7.4) to give 10% homogenate (w/v), and then the homogenates were cool centrifuged at 9000 rpm for 20 min, and supernatants were separated in aliquots and stored at −80°C until determination of oxidative stress markers.

BMI and body weight gain

Body weight gain and BMI of both obese and normal rats groups were recorded at start and end of the experiment and were calculated according to the following equations [25].

$$\text{Body weight gain } (\%) = \left(\frac{W2 - W1}{W1}\right) \times 100.$$

Where W_1 is the animals' weight at start andW_2 is the animals' weight at the end of the experiment.

$$\text{BMI} = \frac{\text{weight}(g)}{\text{nose - anus length}(cm^2)}.$$

Biochemical, myokine, and cytokine determinations

Serum glucose level was determined, at the time of blood sampling, using reagent kits purchased from Vitro Scient Co. (Cairo, Egypt). Serum insulin level was performed using ELISA (Dynatech Microplate Reader Model MR 5000, Canada) and reagent kits purchased from Immunospec Co, Ltd, No. 7018 Owensmouth Ave, Suite 103, Canoga Park, United States. Creatinine and urea levels were determined using reagent kits purchased from Vitro Scient Co. (Cairo, Egypt). Serum leptin concentration was measured using reagent kits (EL2001-1) purchased from Assaypro (USA). Irisin and tumor necrosis factor α (TNFα) levels were measured using reagent kits (SG-10179 and SG-10127, respectively) purchased from SinoGeneClon Biotech Co. (Hang Zhou, China). Serum alanine aminotransferase (ALAT) and aspartate aminotransferase (ASAT) activities were determined using reagent kits purchased from Vitro Scient (Cairo, Egypt). Serum gamma-glutamyl transferase (GGT) activity was measured using reagent kits purchased from BioSystems (Spain). Alkaline phosphatase (ALP) activity was assayed using reagent kits purchased from Diagnostic Systems GmbH (IVD Alte Strasse 9 65558 Holzheim, Germany). Total proteins and albumin, total cholesterol, triglycerides, and high-density lipoprotein (HDL) cholesterol levels were determined with reagent kits obtained from Spectrum Diagnostics (Cairo, Egypt). Low-density lipoprotein (LDL) cholesterol level was calculated according to equation of McNamara *et al*. [28]. Very Low-density lipoprotein (VLDL) cholesterol concentration was calculated according to the equation of Friedewald *et al*. [29]. Atherogenic indices (AIP, CRI-I, and CRI-II) were calculated according to Aboulgasem and Azab [30]. Creatine kinase and lactate dehydrogenase activities were estimated according to the kinetic methods using reagent kits purchased from Diagnostic Systems GmbH. Serum PON1 activity was determined according to the kinetic spectrophotometric chemical method described by Eckerson *et al*. [31] using a substrate buffered mixture [Paraoxon (1.0 mol/l), $CaCl_2$ (1.0 mmol/l), glycin buffer (50 mmol/l)]. Under the aforementioned system, PONase can hydrolyze paraoxon (sigma) to ρ-nitrophenol and diethylphosphate. The rate of paraoxon hydrolysis can be measured spectrophotometrically at 405 nm and 37°C by monitoring the increase of absorbance at zero time and each 2-min interval for 10 min. All samples were run in duplicate. The average value was used for activity calculation using a molar extinction coefficient of 18, 300 M/cm for p-nitrophenol. Results are expressed as U/l for PON1 activity (nmole paraoxon hydrolyzed per minute).

Oxidative stress markers of liver and heart tissues

Tissue reduced glutathione (GSH), superoxide dismutase (SOD), catalase (CAT), and nitric oxide (NO) levels were determined using reagent kits obtained from Biodiagnostic Co. (Giza, Egypt). Lipid peroxidation level was estimated chemically according to the method described by Ruiz-Larrea *et al*. [32] on the basis of malondialdehyde (MDA) reaction with thiobarbituric acid, which forms a pink complex that can be measured photometrically. In this method, 0.5 ml of liver homogenate supernatant (1 g Liver or heart tissue was homogenized in 10 ml phosphate buffer pH 7.4 and cool centrifuged at 5000 rpm for 10 min) was added to 4.5 ml of working reagent (0.8 g thiobarbituric acid was dissolved in 100 ml percloric acid 10% and mixed with 20% trichloroacetic acid in volume ratio 1–3, respectively). In a boiling and shaking water bath, the sample-reagent mixture was left for 20 min, and then carried out to cool at room temperature, and centrifuged for 5 min at 3000 rpm. The absorbance of the clear pink supernatant was measured photometrically at 535 nm against reagent blank (0.5 ml of distilled water +4.5 ml of working reagent).

RNA extraction and reverse transcription PCR

Total RNA was isolated from liver samples using BIOZOL reagent purchased from Bioer Technology Co. Ltd. (Hang zhou, China) following manufacturer's instructions. Reverse transcription (RT) of total RNA to cDNA was performed by mixing 1 μg of total RNA, 1.5 μl from 10 μ? oligo (dT) (Thermo Fisher Scientific Inc., Waltham, Massachusetts, USA), 2 μl of 10 mM dNTP mix (Promega Corporation, Madison, Wisconsin, USA), 4 μl of 25 mM MgCl2 (Promega Corporation), 2 μl of ×10 RT buffer (SibEnzyme Ltd, Novosibirsk, Russia), 2 μl RNase-inhibitor (Promega Corporation), and 7.5 μl RT-enzyme (M-Mul V)

(SibEnzyme Ltd.). The volume of this reaction mixture was completed to 25 µl of DEPC-treated water and incubated at 70°C for 10 min, then at 37°C for 10 min, and 42°C for 1 h, followed by final extension stage at 72°C for 10 min [33]. cDNA product was kept at −20°C. RT was carried out in Biometra thermocycler (Analytik Jena Company, Göttingen, Germany).

Quantitative real-time PCR analysis

PCR was performed with specific primers for FNDC5 (F:

3′CTTCATTCTCCGCTGGTCCCTG 5′; R: 5′ CAGATGCAAGCAGCCGTCTCAG 3′) and GAPDH (F: 3′TCAAGAAGGTGGTGA AGC-AG-5′; R: 5′AGGTGGAAGAAT GGGAGTTG-3′) as a house-keeping gene. The primers were obtained from Sigma Co. (Sigma Aldrich, Egyptian International Center for Import, Cairo, Egypt). All PCR reactions were performed using Maxima SYBR Green qPCR Master Mix (Bioline, London, UK) and were carried out using Agilent Mx3005P QPCR System (Agilent Technologies Co., Santa Clara, California, USA). Mixtures were prepared in a total volume of 20 µl containing 1 µg of cDNA sample, 0.8 µl of forward primer, 0.8 µl of reverse primer, 10 µl of Sybr Green mastermix, and the volume was completed to 20 µl with RNase/DNase-free sterile water. The PCR reaction consisted of one cycle involved initial denaturation at 95°C for 10 min, followed by 40 cycles of 15 s at 95°C, 30 s at 62°C, and 30 s at 72°C. Each sample was analyzed in triplicate. Differences in gene expression between groups were calculated using the $^{\triangle\triangle}$Ct (cycle threshold, Ct) method [34], which were normalized against GAPDH and expressed as relative mRNA levels compared with controls. Ct indicates the fractional cycle number at which the amount of amplified target reaches a fixed threshold.

Histopathology

Portions from the liver of different groups were sectioned into 5-µm-thick paraffin sections, stained with hematoxylin and eosin [35], and investigated by a light microscope.

Statistical analysis

Comparisons between means were carried out using one-way analysis of variance followed by post-hoc (Tukey) multiple comparisons test at significance level of *P* value more than or equal to 0.05 according to Steel and Torrie [36]. This was carried out using statistical analysis system (SAS) program software; copyright (c) 1998 by SAS Institute Inc. (Cary, North Carolina, USA).

Results

In vitro estimation results' yield, total phenolic compounds, radical scavenging activity, and reducing power of MAE are shown in Fig. 1a, b.

BMI was not disturbed in MAE-treated healthy animals, whereas obese-modeled rats recorded a significant elevation compared with those of healthy control. Moreover, treatment of obese rats with MAE led to a significant reduction in BMI compared with obese rat group (Fig. 2).

Treatment of healthy animals with MAE neither deteriorated the activities of serum ALAT, ASAT, GGT, and ALP nor the levels of total proteins, albumin, globulin, A/G ratio, creatinine and urea; in contrast, obese animal group recorded a significant increase in the activity of ALAT, ASAT, GGT, and

Figure 1

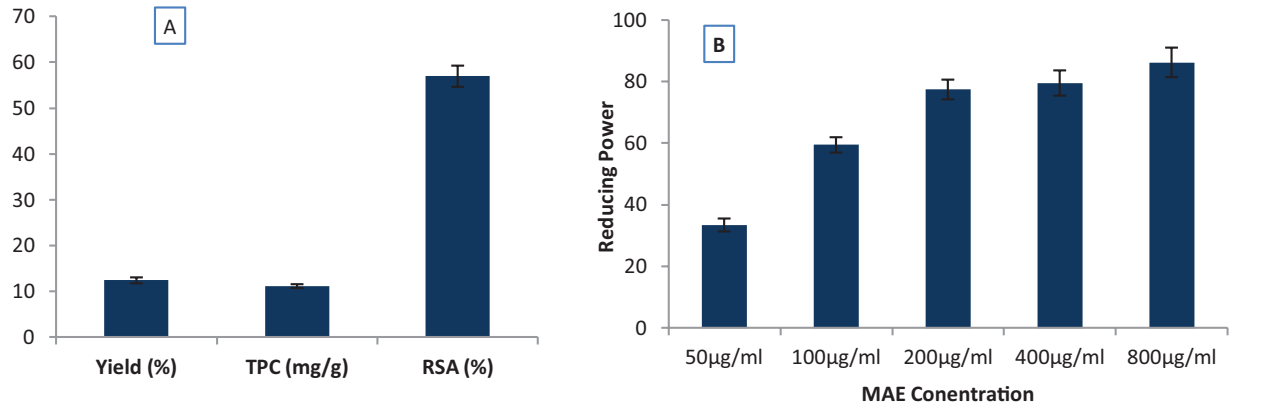

(a) Yield, TPC, and RSA of MAE (mean of three replicates±SEM). (b) Reducing power of MAE (mean of three replicates±SEM). MAE, Moringa aqueous extract; RSA, radical scavenging activity; TPC, total phenolic compounds.

Figure 2

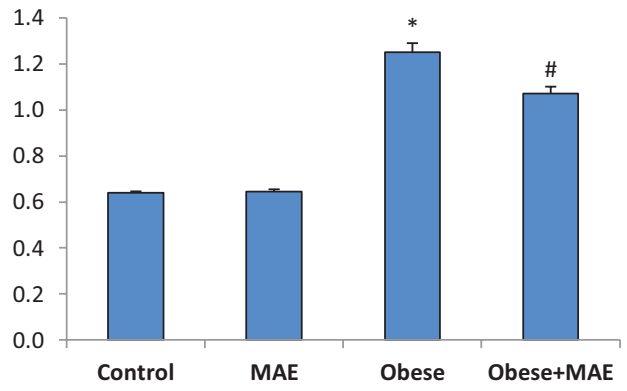

BMI of control, obese, and MAE-treated rats. The data represented as mean±SEM. *Significant from healthy group, #Significant from obese group. MAE, Moringa aqueous extract.

Table 1 Liver and kidney functions of control, obese, and Moringa aqueous extract-treated animals groups

	Control	MAE	Obese	Obese–MAE
ALAT (U/l)	22±1.43	22±0.96	55±2.4*	38±2.5#
ASAT (U/l)	51±1.9	47±4.1	136±9.9*	110±8.3#
GGT (U/l)	6 ±0.44	5.8±0.32	9.8±0.81*	5.9±0.45#
ALP (U/l)	273±6	261±9	291±14	280±15
Albumin (g/dl)	3.95 ±0.41	4.08±0.33	4.2 ±0.18	5.2±0.21#
Proteins (g/dl)	5.8 ±0.56	5.9±0.46	5.9±0.28	8.1±0.48#
Creatinine (mg/dl)	1.02 ±0.083	0.867 ±0.033	0.917 ±0.142	1.08±0.18
Urea (mg/dl)	45±1.68	42±2.27	42±3.97	44±2.81

The data are represented as mean±SEM, and subjected to one-way analysis of variance followed by post-hoc (Tukey) test at *P* value less than or equal to 0.05. ALAT, alanine aminotransferase; ALP, alkaline phosphatase; ASAT, aspartate aminotransferase; GGT, gamma-glutamyl transferase; MAE, Moringa aqueous extract. *Statistically significant from healthy group. #Statistically significant from obese group.

ALP, but did not disturb the other measurements when MAE-treated group was compared with the healthy group. Fortunately, treatment of the obese rat group with MAE resulted in improvements in the values of ALAT, ASAT, GGT, ALP, albumin, and total proteins level compared with obesity rat group (Table 1).

Comparing with the control group, administration of rats with MAE did not disturb serum glucose, insulin, lipid profile, atherogenic indices, creatine kinase, and lactate dehydrogenase values, whereas obese rat group revealed a marked deterioration in these measurements. Promisingly, treatment of obese rats with MAE resulted in a significant improvement in the mentioned parameters (Table 2).

Similarly, neither serum irisin, TNFα, leptin, nor PON1 values were disturbed after MAE treatment of healthy animals, whereas obese-modeled ones

Table 2 Serum glucose, insulin, lipid profile, atherogenic indices, creatine kinase, and lactate dehydrogenase of control, obese, and Moringa aqueous extract-treated animal groups

	Control	MAE	Obese	Obese–MAE
FBS (mg/dl)	67±2.44	68±4.59	134±3.43*	100±9.94*#
Insulin (mIU/l)	49±1.2	48±1.5	27±0.9*	33±1.4*#
TC (mg/dl)	76±3.3	72±3.3	127±5.74*	115±5.23*#
TG (mg/dl)	71±3.28	66±5.03	93±5.44*	81±3.44
HDL-C (mg/dl)	49±2.42	47±1.71	35±3.3*	38±2.6*
LDL-C (mg/dl)	25±1.48	25±1.57	72±2.7*	53±3.82*#
VLDL (mg/dl)	14.17 ±0.6	13.33 ±1.02	18.83 ±1.14*	16.33±0.71
Atherogenic index	1.48 ±0.09	1.44 ±0.15	2.9±0.52*	2.18±0.19
CRI-I	1.59 ±0.08	1.53 ±0.06	3.92 ±0.57*	3.09±0.31*
CRI-II	0.53 ±0.03	0.54 ±0.05	2.27 ±0.38*	1.45±0.17*#
Total CK (U/l)	41±5.8	40±4.2	123±4.1*	106±12*
LDH (U/l)	1081 ±38	1056±34	1898±71*	1520±56*#

The data are represented as mean±SEM, and were subjected to one-way analysis of variance followed by post-hoc (Tukey) test at *P* value less than or equal to 0.05. CK, creatine kinase; HDL-C, high-density lipoprotein cholesterol; LDH, lactate dehydrogenase; LDL-C, low-density lipoprotein cholesterol; MAE, Moringa aqueous extract; TC, total cholesterol; TG, triglycerides; VLDL, very low-density lipoprotein. *Statistically significant from healthy group. #Statistically significant from obese group.

Figure 3

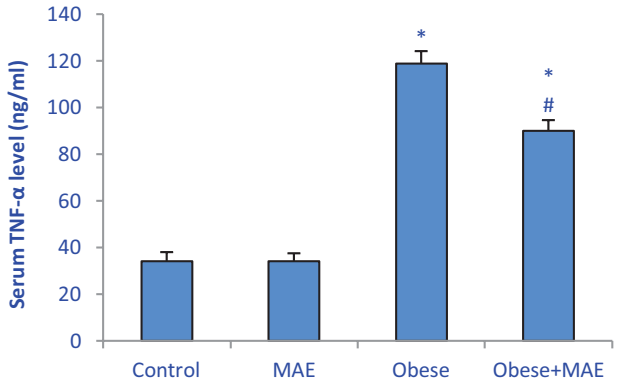

Serum TNFα value of nonobese and obese adult male albino rats treated with MAE. The data are represented as mean±SEM. *Significant from healthy group, #significant from obese group. MAE, Moringa aqueous extract; TNFα, tumor necrosis factor α.

showed a significant reduction in serum irisin and PON1 coupled with a significant rise in both TNFα and leptin levels compared with control group. Interestingly, treatment of obese animals with MAE significantly downregulated the serum TNFα and leptin levels and upregulated serum irisin and PON1 values (Figs 3–6).

Compared with normal rats, MAE-administrated group showed neither adverse oxidative stress voltage

(NO and MDA) nor the antioxidant battery (GSH, SOD, and CAT) of liver and heart, whereas obese rats recorded a significant reduction in GSH, SOD, and CAT values coupled with a significant increase in NO and MDA levels. Interestingly, treatment of obese rats with MAE resulted in a marked decrease in MDA and NO levels, matched with a marked rise in the GSH, SOD, and CAT values compared with the corresponding values of obese rat group (Table 3).

The obtained result showed insignificant reduction in skeletal muscle FNDC5 mRNA expression in obese rats as compared with the control group, although a marked upregulation was observed in obese rat treated with Moringa in comparison with obese rats. Additionally, oral administration of healthy rats with MAE recorded insignificant change in the expression of FNDC5 when compared with the control group. Favorably, oral treatment of obese group with MAE

Figure 4

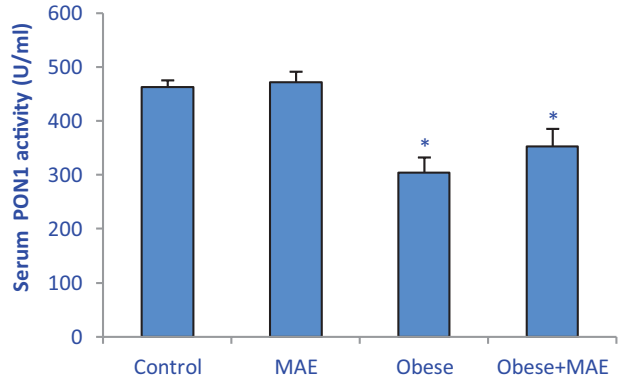

Serum PON1 activity of nonobese and obese adult male albino rats treated with MAE. The data are represented as mean±SEM. *Significant from healthy group, #significant from obese group. MAE, Moringa aqueous extract; PON1, paraoxonase-1.

Figure 5

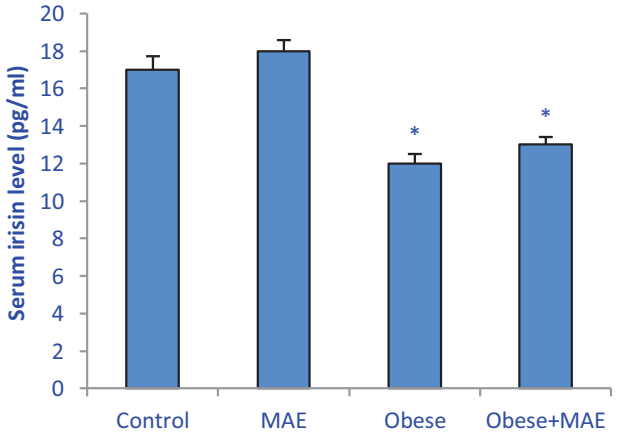

Serum irisin of nonobese and obese adult male albino rats treated with MAE. The data are represented as mean±SEM. *Significant from healthy group, #significant from obese group. MAE, Moringa aqueous extract.

Figure 6

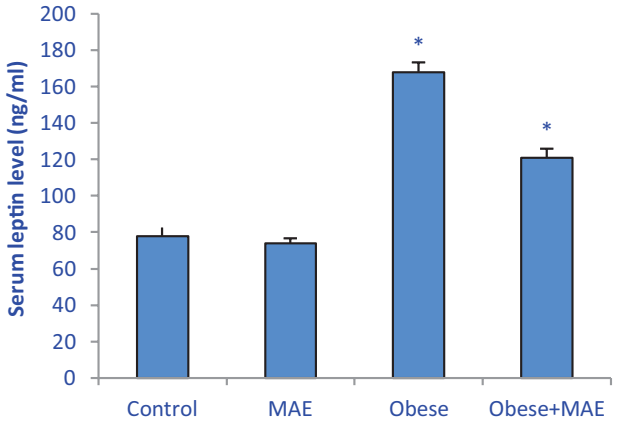

Serum leptin of nonobese and obese adult male albino rats treated with MAE. The data are represented as mean±SEM. *Significant from healthy group, #significant from obese group. MAE, Moringa aqueous extract.

Table 3 Hepatic and cardiac oxidative markers (glutathione, superoxide dismutase and catalase, malondialdehyde, and nitric oxide) of control, obese, and Moringa aqueous extract-treated animal groups.

	Control	MAE	Obese	Obese–MAE
Liver				
GSH (mg/g tissue)	112±3.44	114±2.65	66±3.08*	85±5.4*#
SOD (U/g tissue)	984±45	993±14	608±35*	764±26*
CAT (U/g tissue)	91±2.98	92±4.56	62±3.53*	67±6.6*
MDA (nmol/g tissue)	154±8	152±6.8	290±24*	213±16*#
NO (μmo1/g tissue)	60±2.29	58±2.67	107±7*	89±4.95*
Heart				
GSH (mg/g tissue)	77±2.44	80±2.34*	54±5.5*	70±4.43#
SOD (U/g tissue)	74142±2877	74928±4003	51714±3179*	59185±2358*
CAT (U/g tissue)	9.9±0.098	10.3±0.016	6.8±0.188*	9.3±0.235
MDA (nmol/g tissue)	67±5.5	64±3.09	102±3.18*	86±2.023*#
NO (μmo1/g tissue)	29±0.980	28±0.894	60±8.67*	46±9.1

The data are represented as mean±SEM; subjected to one-way analysis of variance followed by post-hoc (Tukey) test at *P* value less than or equal to 0.05. CAT, catalase; GSH, glutathione; MAE, Moringa aqueous extract; MDA, malondialdehyde; NO, nitric oxide; SOD, superoxide dismutase. *Statistically significant from healthy group. #Statistically significant from obese group.

upregulated the expression of FNDC5 as compared with obese group (Figs 7–11).

Figure 7

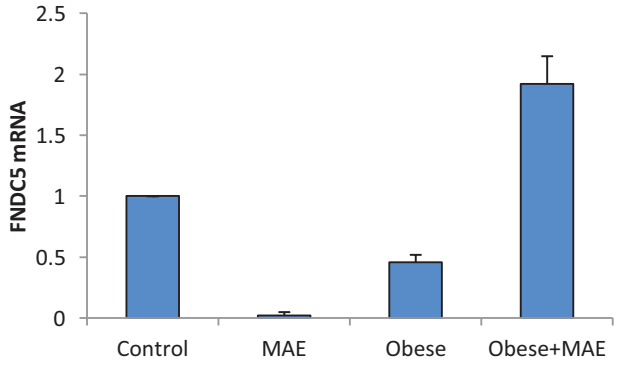

Fibronectin type III domain-containing protein 5 (FNDC5) expressed in muscle of nonobese and obese adult male albino rats treated with MAE. The data represented as mean±SEM. *Significant from healthy control group, #significant from obese group. MAE, Moringa aqueous extract.

Discussion

This study declared that MAE neither disturbed liver, kidney, or heart physiological functions [37]; oxidative status [16]; BMI; glucose; insulin; lipid profile; nor atherogenic indices [38], reflecting a physiological safe effect of MAE. Obese animals showed a marked increase in ALAT, ASAT, GGT, and ALP levels without any effect on serum urea, creatinine, and proteins. Liver histological structure was also deteriorated, as was suggested before [39,40]. Fat accumulation and lipid peroxidation in both membranes and cytosol of hepatocytes caused escaping of liver enzymes from the hepatocyte-cytosol into the circulation [41], indicating disruption in hepatocytes integrity and function [42]. In addition, partly infiltrated inflammatory cells, macrosteatosis/microsteatosis, and inflammation features were observed in obese livers, confirming that effect [43].

Figure 8

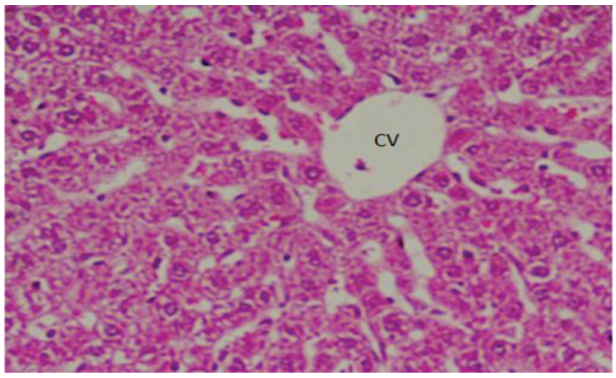

Section of the liver of healthy control rats showing normal histological structure of hepatic lobules and central vein (cv) (hematoxylin and eosin, ×400).

Figure 9

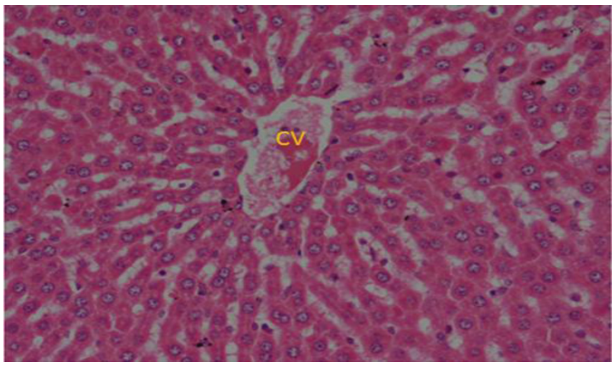

Section of the liver of healthy rats treated with MAE (400 mg/kg body weight) showing normal histological structure of hepatic lobules and central vein (cv) (hematoxylin and eosin, ×400). MAE, Moringa aqueous extract.

Figure 10

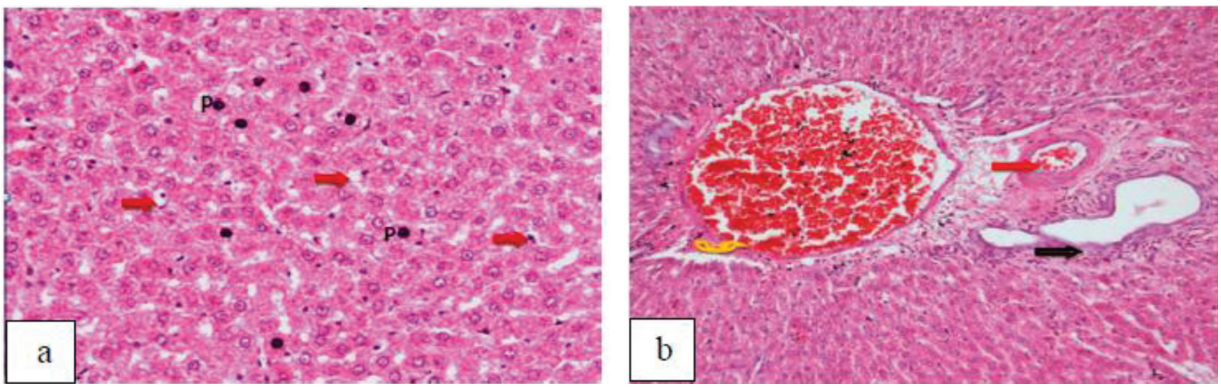

(a) Section of liver of obese-rats showing micro vesicular (red arrow) steatosis and sings of degeneration in the form of pyknosis (P) (hematoxylin and eosin, ×200). (b) Another filed of liver of obese-rats showing dilated, congested portal vein (orange arrow), fibrosis in portal area, dilated bile duct (red arrow) and cellular infiltration around (black arrow) (hematoxylin and eosin, ×100).

Figure 11

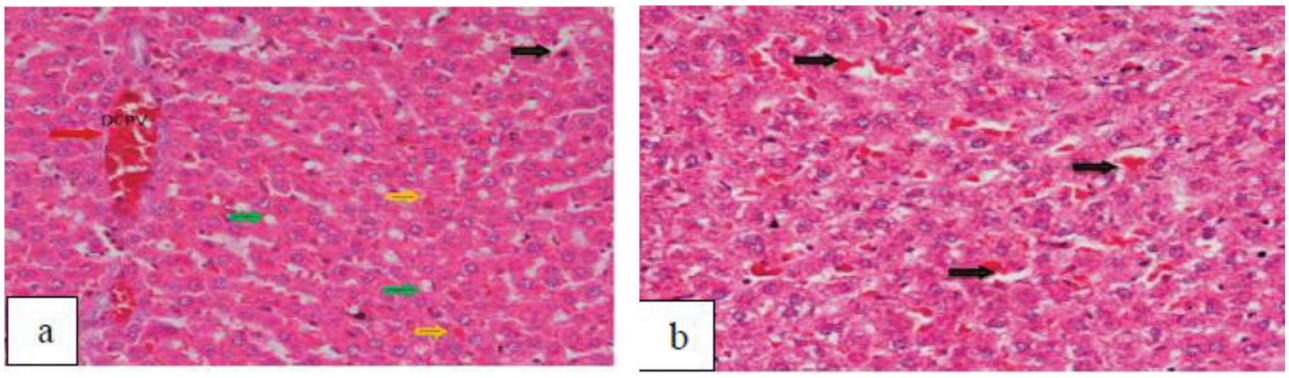

(a) Section of liver of obese-rats treated with MAE (400 mg/kg body weight) showing that the liver still suffering from pathological changes in the form of dilated and congested portal (red arrow). Some singes of degeneration are seen in the form of minute vacuolar degeneration (green arrow) and pyknotic hepatocyte (black arrow) (hematoxylin and eosin, ×200). (b) Another filed of liver of obese rats treated with MAE (400 mg/kg body weight) showing red blood cells in dilated blood sinusoids could be seen (black arrow) (hematoxylin and eosin, ×200). MAE, Moringa aqueous extract.

FNDC5 gene was slightly expressed in healthy MAE-treated rats and markedly expressed in MAE-treated obese ones, reflecting the FNDC5-expressing and irisin-releasing potential of MAE. Both in humans and rodents, the positive correlation of brown fat tissue formation with antiobesity effects suggests a central role of beige adipocyte thermogenesis in whole-body energy metabolism [44]. It was suggested that irisin ameliorates obesity and glucose disorders [45] and that circulating irisin is negatively associated with BMI and percentage of fat mass [46]; in harmony with that, the current study showed that the skeletal muscle FNDC5 mRNA expression level was decreased in obese rats, combined with a significant reduction in circulating irisin level. The current study highlights, for the first time, that MAE improved the obesity status by increasing FNDC5 gene mRNA expression and serum irisin level, as a consequence. One or more mechanisms could be proposed; it could be postulated that FNDC5 gene was cleaved under the effect of MAE constituents, resulting in production of the soluble protein 'irisin,' which is responsible for browning of white adipose tissue as well as increment of total body energy expenditure, and secondly, the observed downregulation and upregulation of FNDC5 in obese and Moringa-treated rats, respectively, may be associated with the observed leptin level change in our study because leptin has a regulatory role on FNDC5/irisin as mentioned by Rodriguez *et al.* [47]. FNDC5 mRNA expression may also be induced by elevation of NO level, a second messenger molecule, contractility, and blood flow in the skeletal muscles, as previously reported by Chatterjee *et al.* [48]. Generally, MAE therapy leads to marked improvement in liver and kidney functions, as well as liver histological structures of MAE-treated obese animals, as stated by Yousef *et al.* [49].

Obesity model showed a marked increase in BMI and glucose levels as previously reported [50,51]; this may be owing to intake of excessive calories and the fat accumulation, as there is a direct correlation between the intake of fat and BMI as well as deposition of fat in the liver [52], which is evidenced herein by the raised cholesterol, triglycerides, LDL, and VLDL and atherogenic indexes [43,50]. It was reported that adipose tissue lipids are greatly derived from triglycerides that circulate in blood, especially during feeding on high-fat diet [53]. The disturbed lipid profile in this study also could be owing to the reversed transport of cholesterol from the circulation to the liver [54]; high-fat diet leads to internal disorders of lipid metabolism manifested as hypercholesterolemia, hypertri-glyceridemia, and high LDL [55]. Glycolipid metabolism disorders are associated with major risk factors leading to cardiovascular disease such as atherosclerosis, thrombosis, and blood supply disorders [56]; that is why, the atherogenic indexes were markedly elevated herein our study.

Oxidative stress results from an imbalance between pro-oxidants and antioxidants [57]. The significant reduction in hepatic, renal, and cardiac GSH, SOD, and CAT accompanied with a marked elevation of MDA and NO in obese rats is against the findings of Della Vedova *et al.* [58] and Yang *et al.* [43]. Indeed, elevated production of reactive species is suggested to be resulted by activation of inflammatory cells at the sites of adipose tissue inflammation and hypertrophy [59]. As a positive correlation between BMI and lipid peroxidation was evidenced [26], the increased NO

level could be a consequence of the expression of endothelial NO synthase in subcutaneous adipose tissues [60]. Similarly, the reduction of SOD, CAT, and GSH values could be attributed to the increased oxidative stress after lipid metabolism disorder and excessive ROS generation [43,58]. The marked decrease of irisin and PON1 values and increase of leptin and TNFα levels of obese-rats serum were also confirmed [61,62].

Under oxidative stress, PON1 activity could be inactivated as a result of altered formation and/or release of HDL, or by S-glutathionylation via a redox regulatory mechanism characterized by the formation of mixed disulfide between a protein thiol and oxidized GSH [63]. Leptin is secreted by the adipocytes and over-released during obesity; this could be owing to many factors: the excessive ROS generation, reduced hypothalamic leptin receptor expression [61], or and the extensive progression of the adipocytes; therefore enlargement of adipose tissue. The impaired blood flow results in hypoxia, which leads to necrosis and infiltration of macrophages in adipose tissue [64] and overproduction of adipokines, which include pro-inflammatory TNFα [65]. Moreno-Navarrete *et al.* [66] illustrated that the amount of brownadipose tissue significantly decreased in obesity and was negatively related with BMI. They attributed the decreased irisin level in obese patients to the lower amounts of brown adipocytes in adipose tissue. In agreement with this hypothesis, circulating irisin level was significantly decreased in obese animal group in the current study.Selvakumar and Natarajan [67] attributed the hepatoprotective property of MAE to presence of many bioactive components, mainly, quercetin and kaempferol. MAE-treated obese rats showed a significant improvement in insulin, HDL cholesterol, glucose, BMI, cholesterol, triglycerides, LDL, and VLDL, and atherogenic indices near the control values; this result is against the reports of Tuorkey [68] and Elabd *et al.* [50] The hypolipidemic effect of different medicinal plants has been related to their bioactive components; cholesterol downregulation property of MAE may be owing to flavonoids, which may augment the activity of lecithin acyltransferase, which regulates blood lipids through incorporation of free cholesterol into HDL and transferring it back to VLDL and LDL, which are taken back later in liver cells [69].

The significant decrease in serum leptin coupled with marked elevation of PON1 in MAE-treated obese animals comes in line with Daba *et al.* [61] and Sierra-Campos *et al.* [70]. Leptin antagonizes the effect of insulin and increases inflammation [71] which is confirmed by the rise in both serum TNFα and hepatocardiac oxidative parameters in obese animals. The marked improvement in GSH, SOD, CAT, MDA, and NO of both hepatic and cardiac tissues concomitant with significant decrease in TNFα posttreatment of obese rats with MAE, comes in line with many previous findings [72,73] who attributed that ameliorating role to the presence of large quantities of phenolics and flavonoids, such as quercetin and kaempferol and ascorbic acid in MAE. The large number of bioactive compounds, with a high reducing power and radical scavenging activity, might explain the pharmacological properties of MAE; thus, its bioactive ingredients were found capable of binding to PON1, which leads to increase in maximal velocity of the reaction. Atrahimovich *et al* [74] showed that the polyphenols of MAE bind to an allosteric site on recombinant PON1 and improve the enzyme function and biology. The results of this study indicated the antiobesity potential of MAE may be mediated by improved plasma irisin and skeletal muscle FNDC5, suggesting a scenario in which irisin enhances white adipocyte transdifferentiation (by increasing UCP1) into beige adipocytes, and as a consequence, the capacity of adipose tissue to uptake glucose or to synthesize fatty acids increases, promoting lipid mobilization or burning these fuels (by increasing PGC1α). FNDC5 gene expression was also negatively associated with TNFα, which is a negative regulator of white transdifferentiation to brown adipose tissue [75].

Conclusion

This study demonstrated that circulating MAE possesses antiobesity efficacy that is evidenced through the upregulation of FNDC5 gene expression and increase of the circulating irisin as well as antidyslipidemic battery that protects the body from the complications that are associated with obesity induced by high-fat diet. Furthermore, the current study demonstrated that the extract, to a high extent, reverses the formation of hepatic steatosis and nonalcoholic hepatic disorder.

Financial support and sponsorship

Nil.

Conflicts of interest

There are no conflicts of interest.

References

1 World Health Statistics. Monitoring health for the SDGs, sustainable development goals. Geneva: World Health Organization 2018.

2 NCD Risk Factor Collaboration (NCD-RisC). Trends in adult body-mass index in 200 countries from1975 to 2014: a pooled analysis of 1698 population-based measurement studies with 19·2 million participants. Lancet 2016; 387:1377–1396.

3 Upadhyay J, Farr O, Perakakis N, Ghaly W, Mantzoros C. Obesity as a disease. Med Clin North Am 2018; 102:13–33.

4 Kyrou I, Randeva HS, Tsigos C, Kaltsas G, Weickert MO. Clinical problems caused by obesity. In: Feingold KR, Anawalt B, Boyce A, Chrousos G, de Herder WW, Dungan K, *et al.* editors. Endotext [Internet]. South Dartmouth, MA:MDText.com, Inc.; 2018. p. 2000–2011.

5 Garrow JS, Webster J. Quetelet's index (W/H2) as a measure of fatness. Int J Obes (Lond) 1985; 9:147–153.

6 Boström P, Wu J, Jedrychowski MP, Korde A, Ye L, Lo JC, *et al.* A PGC1-a-dependent myokine that drives brown-fat-like development of white fat and thermogenesis. Nature 2012; 481:463–468.

7 Spiegelman BM. Banting lecture 2012: regulation of adipogenesis: toward new therapeutics for metabolic disease. Diabetes 2013; 62:1774–1782.

8 Heal DJ, Gosden J, Smith SL. A review of late-stage CNS drug candidates for the treatment of obesity. Int J Obes 2013; 37:107–117.

9 Nakayama H, Tanabe K, Bard M, Hodgson W, Wu S, Takemori D, *et al.* The Candida glabrata putative sterol transporter gene CgAUS1 protects cells against azoles in the presence of serum. J Antimicrob Chemother 2007; 60:1264–1272.

10 Rayalam S, Della-Fera MA, Baile CA. Phytochemicals and regulation of the adipocyte life cycle. J Nutr Biochem 2008; 19:717–726.

11 Mahmood KT, Mugal T, Haq IU. *Moringa oleifera*: a natural gift – a review. J Pharma Sci Res 2010; 11:775–781.

12 Kou X, Li B, Olayanju JB, Drake JM, Chen N. Nutraceutical or pharmacological potential of *Moringa oleifera* Lam. Nutrients 2018; 10: E343.

13 Leone A, Spada A, Battezzati A, Schiraldi A, Aristil J, Bertoli S. Cultivation, genetic, ethnopharmacology, phytochemistry and pharmacology of *Moringa oleifera* leaves: an overview. Int J Mol Sci 2015; 16:12791–12835.

14 Stohs SJ, Hartman MJ. Review of the safety and efficacy of *Moringa oleifera*. Phytother Res 2015; 29:796–804.

15 Mbikay M. Therapeutic potential of *Moringa oleifera* leaves in chronic hyperglycemia and dyslipidemia: a review. Front Pharmacol 2012; 3:1–12.

16 Yassa HD, Tohamy AT. Extract of *Moringa oleifera* leaves ameliorates streptozotocin-induced diabetes mellitus in adult rats. Acta Histochem 2014; 116:844–854.

17 Gowrishankar R, Kumar M, Menon V, Divi SM, Saravanan M, Magudapathy P, Panigrahi Kilany M. Inhibition of human pathogenic bacteria by *Moringa oleifera* cultivated in Jazan (Kingdom of Saudi Arabia) and study of synergy to amoxicillin. Egypt Pharm J 2016; 15:38–42.

18 Amaglo NK, Bennett RN, LoCurto RB, Rosa EAS, LoTurco V, Giuffrid A, *et al.* Profiling selected phytochemicals and nutrients in different tissues of the multipurpose tree *Moringa oleifera* L., grown in Ghana. Food Chem 2010; 122:1047–1054.

19 Lako J, Trenerry VC, Wahlqvist M, Wattanapenpaiboon N, Sotheeswaran S, Premier R. Phytochemical flavonols, carotenoids and the antioxidant properties of a wide selection of Fijian fruit, vegetables and other readily available foods. Food Chem 2007; 101:1727–1241.

20 Khalafalla MM, Abdellatef E, Dafalla HM, Nassrallah AA, Aboul-Enein KM, Lightfoot DA. Active principle from *Moringa oleifera* Lam leaves effective against two leukemias and a hepatocarcinoma. Afr J Biotechnol 2010; 9:8467–8471.

21 Berkovich L, Earon G, Ron I, Rimmon A, Vexler A, Lev-Ari S. Moringa oleifera aqueous leaf extract down-regulates nuclear factor-kappaB and increases cytotoxic effect of chemotherapy in pancreatic cancer cells. BMC Complement Altern Med 2013; 13:212–220.

22 Jayaprakasha GK, Selvi T, Sakariah KK. Antibacterial and antioxidant activities of grape (Vitis vinifera) seed extracts. Food Res Int 2003; 36:117–122.

23 Nogala-Kalucka M, Korczak J, Dratwia M, Lampart-Szczapa E, Siger A, Buchowski M. Changes in antioxidant activity and free radical scavenging potential of rosemary extract and tocopherols in isolated rapeseed oil triacylglycerols during accelerated tests. Food Chem 2005; 93:227–235.

24 Sethiya NK, Trivedi A, Mishra S. The total antioxidant content and radical scavenging investigation on 17 phytochemical from dietary plant sources used globally as functional food. Biomed Prev Nutr 2014; 4:439–444.

25 Shabbir F, Khan S, Yousaf MJ, Khan MA, Rajput TA. Comparison of effect of high fat diet induced obesity and subsequent atorvastatin administration on different anthropometrical measures in Sprague Dawley rats. Pak Armed Forces Med J 2016; 66:699–704.

26 Novelli ELB, Diniz YS, Galhardi CM, Ebaid GMX, Rodrigues HG, Mani F, *et al.* Anthropometrical parameters and markers of obesity in rats. Lab Anim 2007; 41:111–119.

27 Pekkala S, Wiklund PK, Hulmi JJ, Ahtiainen JP, Horttanainen M, Pöllänen E, *et al.* Are skeletal muscle FNDC5 gene expression and irisin release regulated by exercise and related to health?. J Physiol 2013; 591:5393–5400.

28 McNamara JR, Cohn JS, Wilson PW, Schaefer EJ. Calculated values for low-density lipoprotein cholesterol in the assessment of lipid abnormalities and coronary disease risk. Clin Chem 1990; 36:36–42.

29 Friedewald WT, Levy RI, Fredrickson D. Estimation of the concentration of low-density lipoprotein cholesterol in plasma, without use of the preparative ultracentrifuge. Clin Chem 1972; 18:499–502.

30 Aboulgasem GJ, Azab AE. The potential protective effects of pomegranate juice against (s)-(–)-1-methyl-2-(3-pyridyl) pyrrolidine (+)-bitartrate salt induced serum biochemical changes in rabbits. Int J Sci Res 2015; 4:360–371.

31 Eckerson HW, Wyte CM, La Du BN. The human serum paraoxonase/aryl-esterase polymorphism. Amer J Hum Genet 1983; 35:1126–1138.

32 Ruiz-Larrea MB, Leal AM, Liza M, Lacort M, de Groot H. In steroids: antioxidant effects of estradiol and 2-hydroxyestradiol on iron-induced lipid peroxidation of rat liver microsomes. Steroids 1994; 59:383–388.

33 Zhang HM, Zhang XL, Zhou X, Li D, Gu JG, Wu JJ. Mechanism linking atherosclerosis and type 2 diabetes: increased expression of scavenger receptor CD36 in monocytes. Chin Med J 2005; 118:1717–1722.

34 Winer J, Jung CK, Shackel I, Williams PM. Development and validation of real-time quantitative reverse transcriptase-polymerase chain reaction for monitoring gene expression in cardiac myocytes in vitro. Anal Biochem 1999; 270:41–49.

35 Drury R, Wallington EA. Preparation and fixation of tissues. In: Drury RAB, Wallington EA, editors. Preparation and fixation of tissues: Carleton's histological technique. 5th ed. Oxford: Oxford University Press 1980. p. 41–54.

36 Steel RG, Torrie JH. Principles and procedures of statistics. New York: McGraw-Hill Book Company; 1960. p. 481.

37 Awodele O, Oreagba IA, Odoma S, da Silva JA, Osunkalu VO. Toxicological evaluation of the aqueous leaf extract of *Moringa oleifera* Lam.(Moringaceae). J Ethnopharmacol 2012; 139:330–336.

38 Oyewo EB, Adeleke EG, Fakunle BP, Iniaghe MO. Blood glucose and lipid reducing activities of the oral administration of aqueous leaf extract of *Moringa oleifera* in Wistar rats. J Nat Sci Res 2013; 3:92–99.

39 Hussein SA, Abdel-Magid AD, Fareed FAE. Biochemical effect of resveratrol on lipids profile and hepatic oxidative stress in experimentally induced obesity in female rats. Benha Vet Med J 2017; 32:67–74.

40 Zhang HMZ. Phytochemical and pharmacological properties of *Capparis spinosa* as a medicinal plant. Nutrients 2018; 10:E116.

41 Navarro MC, Montilla MP, Martin A, Jimenez J, Utrilla MP. Free-radical scavenger and antihepatotoxic activity of rosmarinus-tomentosus. Planta Med 1993; 59:312–314.

42 Shakoori AR, Butt U, Riffat R, Aziz F. Hematological and biochemical effects of danitol administered for two months on the blood and liver of rabbits. Z Angew Zool 1994; 80:165–180.

43 Yang D, Hu C, Deng X, Bai Y, Cao H, Guo J, Su Z. Therapeutic effect of chitooligosaccharide tablets on lipids in high-fat diets induced hyperlipidemic rats. Molecules 2019; 24:E514.

44 Claussnitzer M, Dankel SN, Kim KH, Quon G, Meuleman W, Haugen C, *et al.* FTO obesity variant circuitry and adipocyte browning in humans. N Engl J Med 2015; 373:895–907.

45 Xiong X, Chen D, Sun H, Ding L, Wang J, Chen Q, *et al.* FNDC5 overexpression and irisin ameliorate glucose/lipid metabolic derangements and enhance lipolysis in obesity. Biochim Biophys Acta 2015; 1852:1867–1875.

46 Huh JY, Panagiotou G, Mougios V, Brinkoetter M, Vamvini MT, Schneider BE, Mantzoros CS. FNDC5 and irisin in humans: I. Predictors of circulating concentrations in serum and plasma and II mRNA expression and circulating concentrations in response to weight loss and exercise. Metabolism 2012; 61:1725–1738.

47 Rodriguez A, Becerril S, Méndez-Giménez L, Ramírez B, Sáinz N, Catalán V, *et al.* Leptin administration activates irisin-induced myogenesis via nitric oxide-dependent mechanisms, but reduces its effect on subcutaneous fat browning in mice. Int J Obes 2015; 39:397–407.

48 Chatterjee S, Ganini D, Tokar EJ, Kumar A, Das S, Corbett J, *et al.* Leptin is key to peroxynitrite-mediated oxidative stress and Kupffer cell activation in experimental non-alcoholic steatohepatitis. J Hepatol 2013; 58:778–784.

49 Yousef FMA, Khattab HAH, Sindi HAA. Effectiveness of *Moringa oleifera* L. leaves extract against methotrexate-induced acute hepatotoxicity in male rats. Int J Pharmacol 2018; 14:1029–1037.

50 Elabd EMY, Morsy SM, Elmalt HA. Investigating of *Moringa oleifera* role on gut microbiota composition and inflammation associated with obesity following high fat diet feeding. J Med Sci 2018; 6:1359–1364.

51 Zhang X, Song Y, Ding Y, Wang W, Liao L, Zhong J, *et al.* Effects of mogrosides on high-fat-diet-induced. Molecules 2018; 23:1894.

52 Rodrigues A, Pereira PC, Vicente AF, Brito JA, Bernardo M, Mesquita MF. Food intake, body mass index and body fat mass in elderly. Asian J Clin Nutr 2012; 4:107–115.

53 Fruchart JC, Brewer HB, Leitersdorf E. Consensus for the use of fibrates in the treatment of dyslipoproteinemia and coronary heart disease. Fibrate Consensus Group. Am J Cardiol 1998; 81:912–917.

54 Raveh O, Pinchuk I, Fainaru M, Lichtenberg D. Kinetics of lipid peroxidation in mixture of HDL and LDL, mutual effects. Free Radic Biol Med 2001; 31:1486–1497.

55 Akiyama T, Tachibana I, Shirohara H, Watanabe N, Otsuki M. High-fat hypercaloric diet induces obesity, glucose intolerance and hyperlipidemia in normal adult male wistar rat. Diabetes Res Clin Pract 1996; 31:27–35.

56 Niroumand S, Khajedaluee M, Khadem-Rezaiyan M, Abrishami M, Juya M, Khodaee G, Dadgarmoghaddam M. Atherogenic index of plasma (AIP): a marker of cardiovascular disease. Med J Islam Repub Iran 2015; 29:240.

57 Jain PG, Patil SD, Haswani NG, Girase MV, Surana SJ. Hypolipidemic activity of *Moringa oleifera* Lam., Moringaceae, on high fat diet induced hyperlipidemia in albino rats. Rev Brasil Farmacogn 2010; 20:969–973.

58 Della Vedova MC, Muñoz MD, Santillan LD, Plateo-Pignatari MG, Germanó MJ, Tosi MER, *et al.* A mouse model of diet-induced obesity resembling most features of human metabolic syndrome. Nutr Metab Insights 2016; 9:93–102.

59 Esposito LA, Melov S, Panov A, Cottrell BA, Wallace DC. Mitochondrial disease in mouse results in increased oxidative stress. Proc Natl Acad Sci 1999; 96:4820–4825.

60 Elizalde M, Ryden M, van Harmelen V, Eneroth P, Gyllenhammar H, Holm C, *et al.* Expression of nitric oxide synthases in subcutaneous adipose tissue of non-obese and obese human. J Lipid Res 2000; 41:1244–1251.

61 Daba MH, Elmasry A, El-karef AA. Effect of *Moringa oleifera* with and without metformin on an experimental model of metabolic syndrome in rats. Int J Adv Res 2015; 3:1624–1632.

62 Hou N, Liu Y, Han F, Wang D, Hou X, Hou S, Sun X. Irisin improves perivascular adipose tissue dysfunction via regulation of the heme oxygenase-1/adiponectin axis in diet-induced obese mice. J Mol Cell Cardiol 2016; 99:188–196.

63 Rozenberg O, Aviram M. Glutathionylation regulates HDL-associated paraoxonase 1 (PON1) activity. Biochem Biophys Res Commun 2006; 351:492–498.

64 Wood JJ, Drahota A, Sze K, Van Dyke M, Decker K, Fujii C, *et al.* Brief report: effects of cognitive behavioral therapy on parent-reported autism symptoms in school-age children with high-functioning autism. J Autism Dev Disord 2009; 39:1608–1612.

65 Johnson AR, Milner JJ, Makowski L. The inflammation highway: metabolism accelerates inflammatory traffic in obesity. Immunol Rev 2012; 249:218–238.

66 Moreno-Navarrete JM, Ortega F, Serrano M, Guerra G, Pardo G, Tinahones F, *et al.* Irisin is expressed and produced by human muscle and adipose tissue in association with obesity and insulin resistance. J Clin Endocrinol Metab 2013; 98:769–778.

67 Selvakumar D, Natarajan P. Hepato-protective activity of *Moringa oleifera* Lam leaves in carbon tetrachloride induced hepato-toxicity in albino rats. Pharmacogn Mag 2008; 4:97–98.

68 Tuorkey MJ. Effects of *Moringa oleifera* aqueous leaf extract in alloxan induced diabetic mice. Interv Med Appl Sci 2016; 8:109–117.

69 Farooq F, Rai M, Tiwari A, Khan AA, Farooq S. Medicinal properties of *Moringa oleifera*: an overview of promising healer. J Med Plants Res 2012; 6:4368–4374.

70 Sierra-Campos E, Valdez-Solana MA, Pérez-Velázquez JR, García-Arenas G, Téllez-Valencia A, Avitia-Domínguez C. Moringa oleifera leaves extract regulate the activity of nitric oxide synthases and paraoxonase 1 in diabetic rat. MO J Biorg Org Chem 2018; 2:236–241.

71 Kaur J. A comprehensive review on metabolic syndrome. Cardiol Res Pract 2014 2014:943162.

72 Sankhalkar S, Vernekar V. Quantitative and qualitative analysis of phenolic and flavonoid content in *Moringa oleifera*Lam and Ocimum tenuiflorum L. Pharmacognosy Res 2016; 8:16–21.

73 Goudaa AS, El-Nabarawya NA, Ibrahim SF. Moringa oleifera extract (Lam) attenuates aluminium phosphide-induced acute cardiac toxicity in rats. Toxicol Rep 2018; 5:209–212.

74 Atrahimovich D, Vaya J, Khatib S. The effects and mechanism of flavonoid-rePON1 interactions. Structure-activity relationship study. Bioorg Med Chem 2013; 21:3348–3355.

75 Toh SY, Gong J, Du G, Li JZ, Yang S, Ye J, *et al.* Up-regulation of mitochondrial activity and acquirement of brown adipose tissue-like property in the white adipose tissue of fsp27 deficient mice. PLoS ONE 2008; 3:e2890.